# Numerical simulation of laminar core-annular flow in a 90° bend

S. M. Park, G. Ooms & M. J. B. M. Pourquie
*J.M. Burgerscentrum, Delft University of Technology, Faculty of Mechanical Engineering, Laboratory for Aero- & Hydrodynamics, The Netherlands*

## Abstract

A numerical study, using the volume-of-fluid method, has been made of laminar core-annular flow in a 90° bend. To verify the numerical method we first compared our results for a single-phase flow in a 90° bend with numerical results and experimental data given in the literature. The agreement was good. Thereafter a detailed analysis was made of the velocities and pressures occurring in core-annular flow in a 90° bend. Special attention was given to the influence of the secondary flow perpendicular to the pipe axis. This secondary flow plays an important role in the behaviour of core-annular flow in a curved pipe.

## 1 Introduction

We study the flow of a high-viscosity liquid (oil) surrounded by a low viscosity liquid (water) through a pipe. This core-annular flow is very interesting from a practical and scientific point of view. Much attention has been paid in the literature to core-annular flow. Joseph and Renardy [1] have written a book about it. There are several review articles, see for instance Oliemans and Ooms [2] and Joseph *et al.* [3]. A description of our recent research can be found in Ooms *et al.* [4] and Beerens *et al.* [5].

Most studies about core-annular flow have focused on straight vertical or horizontal pipes. There are not many studies on core-annular flow in a curved pipe. However in practice (for instance during pipeline transport of very viscous oil with water) one has to deal with curved parts in the pipe. Compared to core-annular flow in a straight pipe the flow in a curved one is more complicated.

WIT Transactions on Engineering Sciences, Vol 89, © 2015 WIT Press
www.witpress.com, ISSN 1743-3533 (on-line)
doi:10.2495/MPF150231

The centrifugal force has a strong influence on the flow pattern, causing a secondary flow perpendicular to the pipe axis. Fouling of the pipe wall by oil is more likely to occur than in a straight pipe. Therefore we decided to study core-annular flow in a curved pipe in more detail.

The flow in a curved pipe is three-dimensional. First we analysed single-phase flow in a curved pipe to investigate the curvature effect on such a flow and to be able to compare the results with available experimental and numerical data given in the literature. A 90° bend was chosen as model geometry with a curvature ratio of 1/6. We concentrated in particular on the shift in the location of maximum axial velocity and on the secondary flow velocity components caused by the centrifugal forces. The agreement between our results and the ones given in the literature was good.

Thereafter we extended the study to core-annular flow in a 90° bend. We used the same flow properties as applied by Ooms *et al.* [4] for a straight pipe. In the first calculation we neglected the buoyancy effect (due to the density difference between the core liquid and annular liquid) to study in particular the effect of the centrifugal force on core-annular flow in a bend. Thereafter we took the buoyancy effect into account to analyse the simultaneous effect of buoyancy and centrifugal force on core-annular flow. The same curvature ratio as used for the single-phase flow was applied. We studied in detail the deformation of the core-annular interface, the axial velocity distribution, the secondary flow development and the pressure distribution.

As limited space is available we restrict ourselves in this paper to core-annular flow in a 90° bend. The results for the single-phase flow are not given here, but can be found in the report by Park [6]. In this report also results are given concerning our numerical simulation in a 180° return bend.

## 2 Numerical method

We solved numerically the Navier–Stokes equations for the flow in the core liquid and annular liquid. The chosen flow conditions were such, that the flow in both liquids was laminar. So no turbulence model has been used. Although no turbulence was present, the inertial forces played an important role. At the core-annular interface continuity of velocities and stresses was applied. For our numerical analysis the package OpenFoam version 2.1.1 was used. In order to simulate the flow of two liquids (with different densities) the volume-of-fluid (VOF) method is an important numerical tool. We applied the interFoam solver in the package OpenFOAM which uses the VOF method. The VOF method has the advantage with respect to the Eulerian–Lagrangian approaches (which traces the interface and regrid if the position of the interface changes) that it is able to represent complicated changes in the interface, since it does not depend on re-gridding but can use a stationary grid. The momentum equations for the mixture are according to the VOF method written as

$$\frac{\partial \rho \mathbf{U}}{\partial t} + \nabla \cdot (\rho \mathbf{U} \otimes \mathbf{U}) = -\nabla p + [\nabla \cdot (\mu \nabla \mathbf{U}) + \nabla \mathbf{U} \cdot \nabla \mu] + \rho \mathbf{g} + \int_{\mathbf{\Gamma}} \sigma \, \kappa \, \delta(\mathbf{x} - \mathbf{x_S}) \, \mathbf{n} \, \mathbf{d\Gamma}(\mathbf{x_S}), \quad (1)$$

with

$$\rho = \alpha \rho_o + (1 - \alpha)\rho_w, \quad \mu = \alpha \mu_o + (1 - \alpha)\mu_w. \quad (2)$$

$\mathbf{U}$ is the velocity, $t$ the time, $p$ the pressure, $\rho_o$ the density of the core liquid, $\rho_w$ the density of the annular liquid, $\sigma$ the surface tension, $\Gamma$ the liquid-liquid interface, $\kappa$ the local interfacial curvature, $\mathbf{n}$ the normal to the interface, $\mathbf{g}$ the acceleration due to gravity, $\delta(\mathbf{x} - \mathbf{x_S})$ the three-dimensional Dirac delta function and $\alpha$ the local volume fraction of core liquid. The surface tension is translated to a volume source term which is included in the Navier–Stokes equation as a source term, following the method of Brackbill *et al.* [7]. More details are given by Deshpande *et al.* [8]. OpenFoam applies the finite-volume-method to solve the relevant partial differential equation. The Gauss limited linear V method was used for the advection terms of the velocity components and the Gauss van Leer method for the advection term of the scalar. For the pressure-velocity coupling the PIMPLE scheme was applied. PIMPLE is the merged PISO-SIMPLE (semi-implicit method for pressure linked equations) scheme. The following linear solvers were used: Preconditioned Conjugate Gradient for the pressure, and Preconditioned Bi-Conjugate Gradient for the velocity components. In the axial flow direction of the pipe we used an equidistant, orthogonal and non-stretched grid. In the radial direction we applied a structured mesh for the annulus and an unstructured one for the core. We used 114, 88, and 91 grid cells in radial, circumferential, and axial flow direction, respectively. (For the radial direction we used 44 structured grid cells in the annulus and 48 unstructured grid cells for the core with double-sided refinement of $15\%$. At the center of the core 22 structured grid cells were used). Due to the movement of the core towards the pipe wall we implemented more closely packed grid cells near the wall than in the core region. The boundary conditions for the calculation domain were as follows. On the pipe wall the no-slip boundary condition was imposed. At the inflow cross-section of the pipe the analytical solution of Li and Renardy (see Ooms *et al.* [4]) for perfect core-annular flow was applied. At the outflow cross-section a zero velocity gradient and a fixed value for the (reduced) pressure was imposed. (A back-flow occurred for the zero-gradient pressure condition.) As initial conditions inside the pipe we used again the analytical solution of Li and Renardy for perfect core-annular flow (applied locally).

## 3 Core-annular flow in a 90° bend without buoyancy effect

We used the $90^\circ$ bend configuration as shown in figure 1.

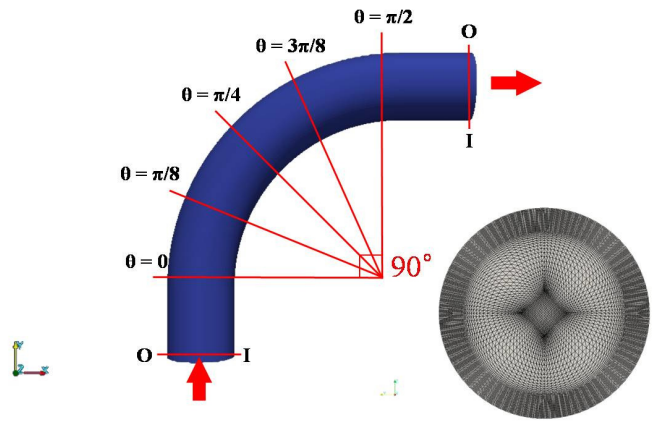


Figure 1: Geometry of the 90° bend. The indicated angles are the location of the cross-sections used in the coming analysis. Also the calculation mesh is shown.

Ooms *et al.* [4] studied horizontal core-annular flow in a straight pipe without buoyancy effect. For our study we applied the same parameters as used by them, but this time for the flow through a 90° bend. The physical parameter values are given in the following table.

| | | |
|---|---|---|
| $\rho_o = 905\,\text{kg/m}^3$ | $\rho_w = 995\,\text{kg/m}^3$ | $\mu_o = 0.601\,\text{kg/ms}$ |
| $\mu_w = 0.001\,\text{kg/ms}$ | $\sigma = 8.54 \cdot 10^{-3}\,\text{kg/s}^2$ | $f = 150\,\text{kg/m}^2$ |
| $R_1 = 0.00372\,\text{m}$ | $R_2 = 0.00476\,\text{m}$ | – |

$\rho_o$ is the core (oil) density, $\rho_w$ the annular liquid (water) density, $\mu_o$ the core viscosity, $\mu_w$ the annular liquid viscosity, $\sigma$ the interfacial tension, $f$ the pressure gradient, $R_1$ the core radius and $R_2$ the pipe radius. The values of the relevant dimensionless groups are given in the next table.

| | | |
|---|---|---|
| $m{=}\frac{\mu_w}{\mu_o}{=}0.00166$ | $a{=}\frac{R_2}{R_1}{=}1.28$ | $\zeta{=}\frac{\rho_w}{\rho_o}{=}1.10$ |
| $K{=}\frac{(f+\rho_o g)}{(f+\rho_w g)}{=}1$ | $J{=}\frac{\sigma R_1 \rho_o}{\mu_o^2}{=}7.96 * 10^{-2}$ | $Re_o{=}\frac{\rho_o V_0(0) R_1}{\mu_o}{=}1.85$ |
| $\kappa_o{=}Re_o\,(a/R_2)^{1/2}{=}0.755$ | – | – |

$V_0(0)$ is the centerline velocity for perfect core-annular flow. $\kappa$ is the Dean number. By neglecting the buoyancy effect we could concentrate on the influence of the centrifugal force on the flow in the curved part of the pipe.

### 3.1 Core shape and position in the pipe

We first studied the location of the core inside the pipe at a number of pipe cross-sections as function of time. In particular we were interested to find out, whether fouling of the pipe wall occurred due to touching of the wall by the oil core. In figure 2 the core position inside the pipe is shown for a number of cross-sections and time steps. It can be seen that the core position is quickly established in time. At the inlet the core has an axisymmetric shape. However further down the pipe the core starts to deform and move to the outer-curved part of the pipe. However it never touches the wall. As we will show later this is due to the pressure build-up in the annular layer which pushes the core from the wall. As oil has a lower density than water we expected that the core would move to the inner-curved part of the pipe. In order to explain this surprising phenomenon we studied the secondary flow perpendicular to the pipe axis.

### 3.2 Axial and secondary flow

In the case of single-phase flow we already found the development of a secondary flow perpendicular to the pipe axis in the curved part of the pipe. This is also the case for core-annular flow, but this time the situation is more complicated. We start with a discussion of the axial velocity distribution in the pipe. In figure 3 this distribution is given for a number of axial positions in the bend. At the inlet the core velocity is nearly constant due to the large viscosity of the oil compared to the water viscosity. In the water annulus the velocity decreases quickly from the core velocity to zero velocity at the pipe wall. However in the curved part of the pipe the core moves to the outer-curved part of the pipe and the core velocity is no longer constant. At this outer-curved part the velocity becomes larger than at the inner-curved part. The highest axial velocity was found at $\theta = \pi/4$: $V_{max} = 0.35$ m/s.

In figure 4 the secondary flow is shown that developed inside the water annulus at $\theta = 3\,\pi/8$. The recirculating flow in the annulus is upward along the core-annular interface and downward along the pipe wall. Of course, at the inlet the secondary flow does not exist. However when the flow enters the curved part of the pipe the secondary flow develops. At first it is rather weak, but it increases in strength on its way to the exit. The maximum magnitude of the secondary flow is of the order $0.05$ m/s (whereas the axial velocity is of the order $0.30$ m/s)). The secondary flow pushes the core and therefore also the position of maximum axial velocity in the direction of the outer-curved part of the pipe.

### 3.3 Pressure distribution

Although the core moves to the outer-curved part of the pipe, it does not touch and foul the pipe wall. This is caused by the pressure build-up at that part of the pipe, as can clearly be seen in figure 5. At the inlet of the pipe the pressure in the core is slightly higher than in annulus due to the interfacial tension. In downstream direction the pressure distribution changes strongly. The pressure at the outer-

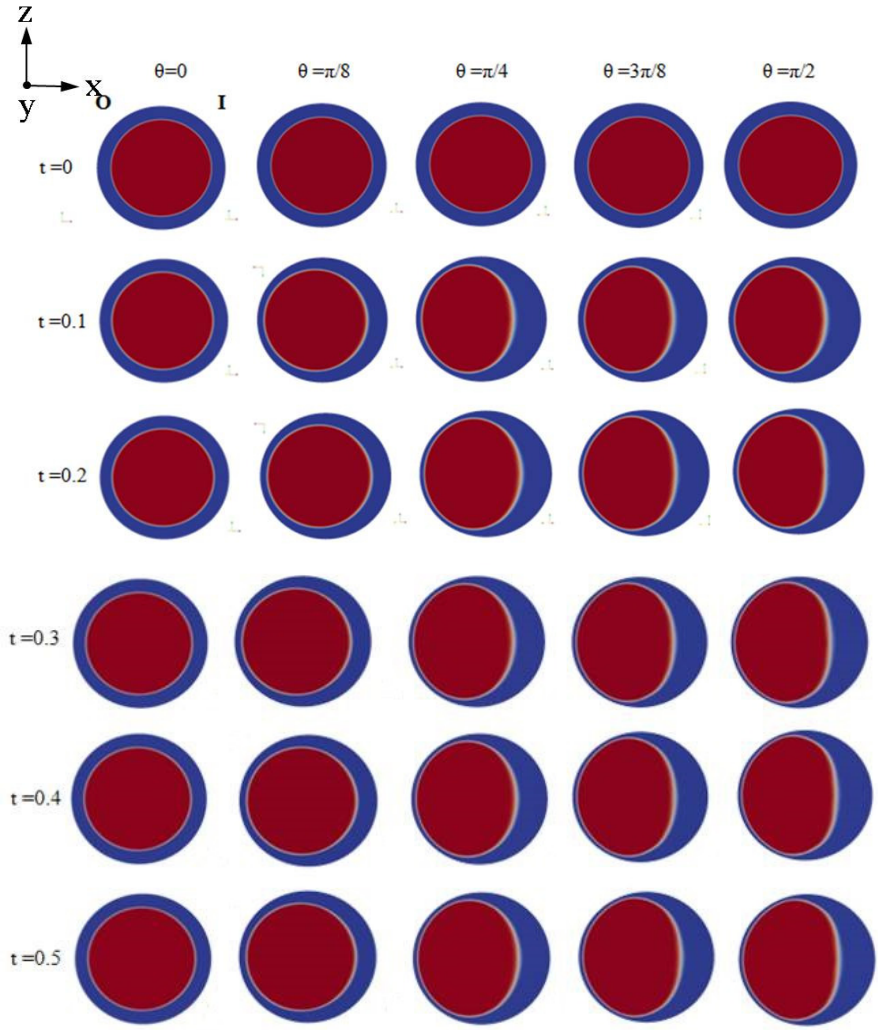


Figure 2: Position of the oil core inside the pipe at five cross-sections as a function of time. (I: inner-curved part of the pipe, O: outer-curved part of the pipe).

curved part of the pipe increases, whereas it decreases at the inner-curved part. So a net force is exerted on the core, pushing it away from the outer-curved part. This is the reason that fouling does not occur, although the annular film at the outer-curved part becomes rather thin.

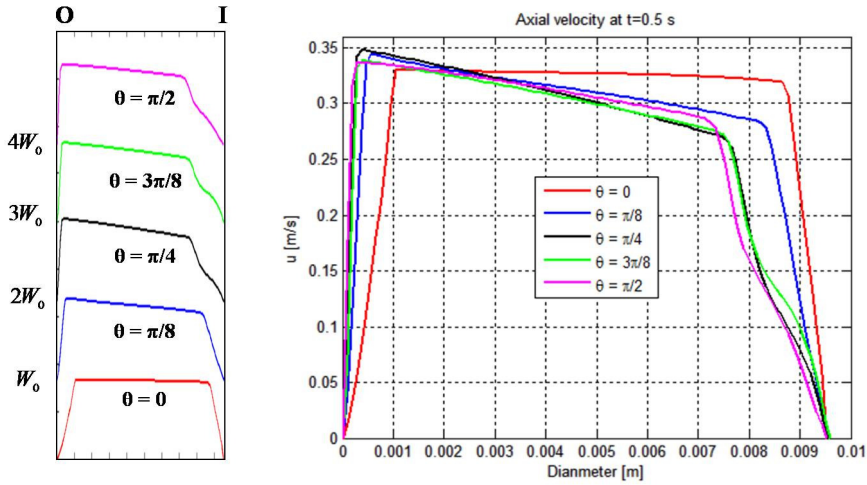


Figure 3: Axial velocity distribution from O to I for five cross-sections of core-annular flow in a 90° bend. (I: inner-curved part of the pipe, O: outer-curved part of the pipe). To see more clearly the differences between the velocity distributions, these distributions are shown in the left part of the figure with a shift of an arbitrary amount $W_0$ in vertical direction.

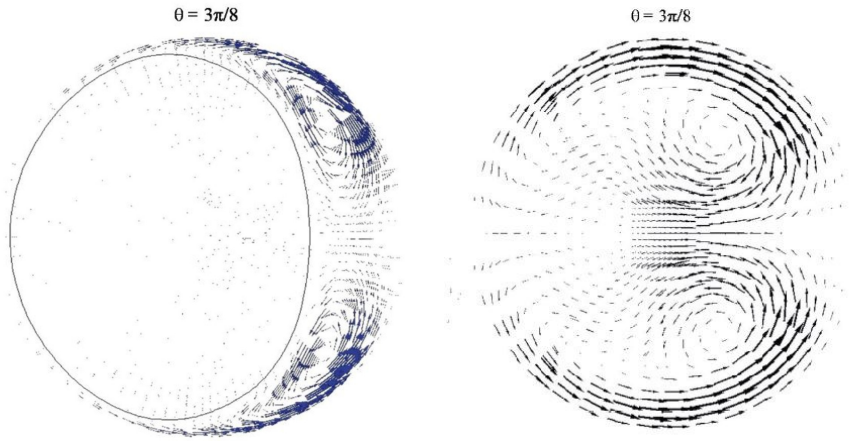


Figure 4: Left: Secondary flow at $\theta = 3\,\pi/8$. As the core viscosity is much larger than the annular liquid viscosity the secondary flow inside the core is extremely weak. Right: For comparison the secondary flow for a single-phase flow (at $Re = 500$) is given.

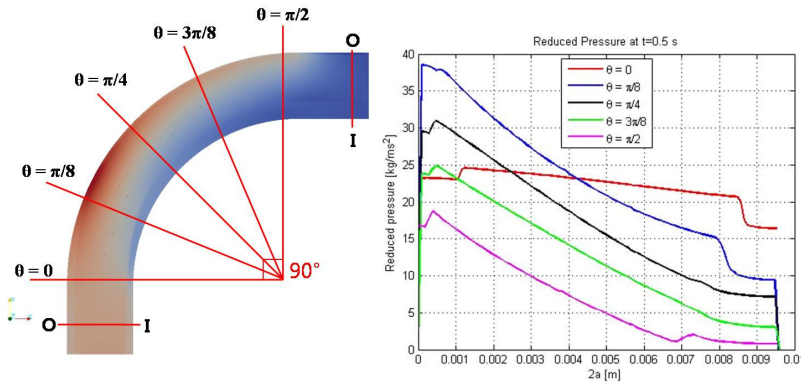


Figure 5: Pressure distribution at $t = 0.5$ from O to I for five cross-sections of core-annular flow in a 90° bend. The nearly horizontal distribution belongs to $\theta = 0$. To see more clearly the differences between the pressure distributions, the other distributions are shown with a shift of an arbitrary amount in vertical direction. The distribution at the top belongs to $\theta = \pi/8$, the next lower distribution to $\theta = \pi/4$, then $\theta = 3\pi/8$ and finally $\theta = \pi/2$. (Only the distribution is important, not the absolute value.)

## 4 Core-annular flow in a 90° bend with buoyancy effect

In this section we present the same study as before, but now with buoyancy effect. The 90° bend is the same as in the foregoing case. We assume that the bend lies in a horizontal plane and that the buoyancy force is perpendicular to it, so perpendicular to the axial flow direction. Apart from the buoyancy force the flow conditions are the same as in the previous case. The centrifugal force is in a horizontal plane in radial direction and the buoyancy force is perpendicular to it. So the combined force is no longer in a horizontal plane, but makes an angle with it.

### 4.1 Core shape and position in the pipe

The core shape and position as function of time for different cross-sections along the pipe are shown in figure 6. At the inlet the core is axisymmetric. However in the curved part of the pipe it moves slightly upwards (due to the buoyancy force) and in the direction of the outer-curved part of the pipe (due to the secondary flow) and the core shape changes significantly. It can be seen that the equilibrium position of the core in the pipe is quickly established. At $\theta = \pi/4$ there is no significant change in the shape and position of the core. Fouling was again not observed.

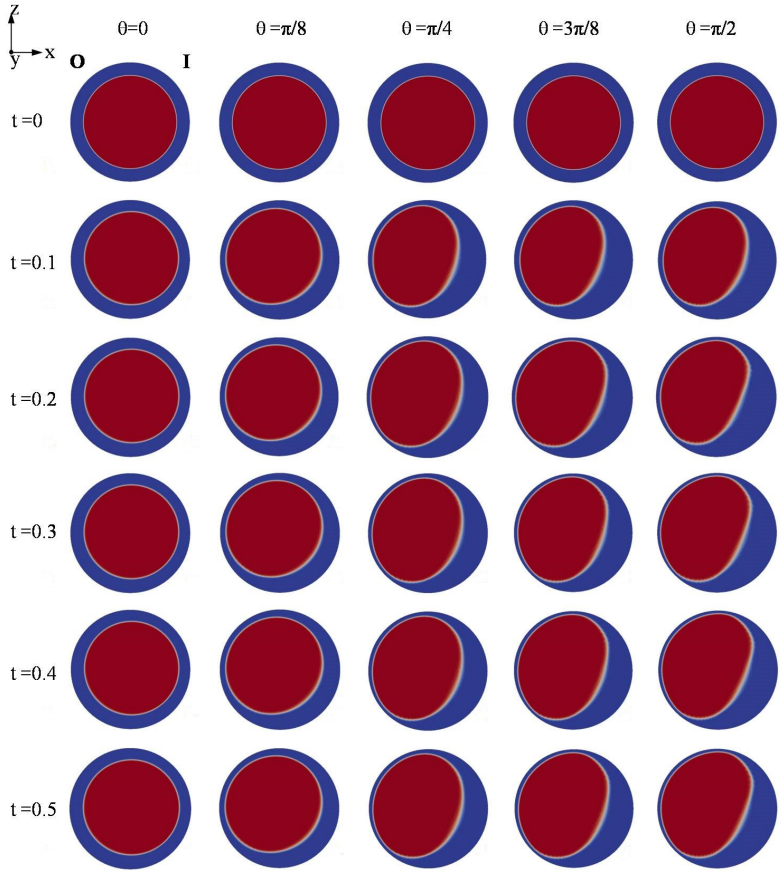


Figure 6: Position of the oil core inside the pipe at five cross-sections as a function of time. (I: inner-curved part of the pipe, O: outer-curved part of the pipe). The core moves to the outer-curved part of the pipe due to the secondary flow and upward under the influence of the buoyancy force.

### 4.2 Axial and secondary flows

The axial velocity distribution is somewhat different from the case without buoyancy. This is due to the fact that the core moves to the outer-curved part of the pipe in a direction that makes an angle (of about 30°) with the horizontal plane. The axial velocity is again highest close to the thinnest part of the annulus. Due to the velocity component of the core in upward direction (under the influence of the buoyancy force) the secondary flow becomes non-symmetrical. The vortex at the top side of the inner-curved part of the pipe becomes weaker than the one at bottom side. The flow at the core-annular interface is again upward at the core-

annular interface and downward along the pipe wall. Only in this case the shear force is larger at the bottom side of the pipe than at the top side. As in the case without buoyancy force the secondary flow pushes the core to the outer-curved part of the pipe and causes the rather strong deformation of the core shape.

### 4.3 Reduced pressure

The result for the reduced pressure (the pressure without buoyancy contribution) is rather similar to the pressure for the case without buoyancy effect, although due to the combined action of centrifugal force and buoyancy force it is slightly larger. The highest values of the pressure are found at the upper side of the outer-curved part of the pipe. The large pressure build-up at the upper side of the outer-curved part of the pipe is responsible for the fact that the core does not touch and foul the pipe wall.

## 5 Conclusion

We have studied two cases of core-annular flow in a 90° bend: first without buoyancy effect and then with buoyancy effect due to the difference in density between the core liquid and annular liquid. In this way we could separate the effect of the centrifugal force and the buoyancy force on the flow. We found that a secondary flow occurred in the annular layer which pushed the core to the outer-curved part of the pipe. Without buoyancy force the movement of the core to the wall was symmetric with respect to the horizontal plane through the centerline of the pipe; for the case with buoyancy effect the core movement was slightly upward and no longer symmetric with respect to this plane. At the outer-curved part of the pipe a high pressure build-up occurred. Therefore the core remained free from the pipe wall and did not foul it.

## References

[1] D.D. Joseph and Y.Y. Renardy, Fundamentals of two-fluid dynamics, part II: Lubricated transport, drops and miscible liquids, Springer-Verlag, New York, (1993).
[2] R.V.A. Oliemans and G. Ooms, Core-annular flow of oil and water through a pipeline, Multiphase Science and Technology (ed. G.F. Hewitt, J.M. Delhaye and N. Zuber), vol. 2, Hemisphere, (1986), Washington.
[3] D.D. Joseph, R. Bai, K.P. Chen and Y.Y. Renardy, Core-annular flows, Ann. Rev. Fluid Mech. **29**, (1999), 65.
[4] G. Ooms, M.J.B.M. Pourquie and J.C. Beerens, On the levitation force in horizontal core-annular flow with a large viscosity ratio and small density ratio, Phys. Fluids **25**, (2013), 032102.

[5] J.C. Beerens, G. Ooms, M.J.B.M. Pourquie and J. Westerweel, A comparison between numerical predictions and theoretical and experimental results for laminar core-annular flow, AIChE Journal **60**(no. 8), (2014), 3046–3056.
[6] S.M. Park, Numerical simulation of core-annular flow in a curved pipe, MSc report of the Technological University Delft, report number: 2625 (MEAH 277). Available as pdf-file from G. Ooms (g.ooms@tudelft.nl).
[7] J.U. Brackbill, D.B. Kothe and C. Zemach, A continuum method for modeling surface tension, J. Comput. Phys. **100**, (1992), 335–354.
[8] S.S. Deshpande, L. Anumolu and M.F. Trujillo, Evaluating the performance of the two-phase flow solver interFoam, Computational Science and Discovery **5**, (2012), 014016.